**Supplemental Material**

**Table S1 – Materials**

| | SOURCE | IDENTIFIER |
|---|---|---|
| **Antibodies** | | |
| **Immunohistochemistry/immunofluorescence** | | |
| Rat anti-mouse/human CD3e (1:300) | Biorad/Serotec | MCA1477 |
| Rat anti mouse-Cd8a (1:300) | ebioscience | 14-0808-80 |
| Rabbit anti-mouse/human Iba1 (1:500) | Wako | 019-19741 |
| Goat anti-Iba1 (1:500) | Abcam | AB-5076 |
| Rabbit anti human/mouse-FoxP3 (1:50) | R&D | MAB8214 |
| Rabbit anti-mouse Olig2 (1:300) | Millipore | AB9610 |
| Chicken anti-GFP (1:5000) | Invitrogen | A10262 |
| Rabbit anti-Neurofilament heavy chain (1:500) | USB | N2160-06L |
| Biotinylated goat anti-rabbit (1:300) | Vector | BA-1000 |
| Biotinylated goat anti-rat (1:300) | Vector | BA-9400 |
| Donkey anti-rabbit Cy3 (1:200) | Jackson Immuno | 711-165-152 |
| Donkey anti-goat 647 (1:200) | Jackson Immuno | 705-605-147 |
| Donkey anti-chicken 488 (1:200) | Jackson Immuno | 703-545-155 |
| | | |
| **ULBP3 binding studies** | | |
| hIgG1-Fc-APC | R&D Systems | FAB110A |
| *Anti-human* | | |
| CD3-BV650 | BioLegend | 317324 |
| CD19-BV510 | BioLegend | 363020 |
| CD14-BV421 | BioLegend | 325628 |
| CD16-FITC | BioLegend | 360716 |
| CD56-PE/Cy7 | BioLegend | 318318 |
| CD163-PE | R&D Systems | FAB1607P |
| *Anti-mouse* | | |
| NKp46-BV711 | BioLegend | 137621 |
| Cd3-BV510 | BioLegend | 100234 |
| Cd19-BV421 | BioLegend | 115538 |
| Ly-6G-FITC | BioLegend | 127606 |
| F4/80-PE/Cy7 | BioLegend | 123114 |
| | | |
| **Flow cytometry** | | |
| Cd45-Alexa Fluor 700 | Biolegend | 30-F11 |
| Cd3-BV711 | Biolegend | 17A2 |
| Cd4-BV786 | Biolegend | RM 4-5 |
| Cd8-PerCP/Cy5.5 | Biolegend | 53-6.7 |
| Pd1-BV421 | Biolegend | 29F.1A12 |
| Tim3-APC | Biolegend | RMT3-23 |
| Cd19-PECy7 | BD | 1D3 |
| Cd274-PE | Biolegend | 10F.69G2 |
| Cd274-BV421 | BD | MIH5 |
| Ly6C-FITC | Biolegend | HK1.4 |
| Ly6G-PE-CF594 | BD | 1A8 |
| Cd11b-PECy7 | eBioscience | M1/70 |
| Cd11c-BV605 | Biolegend | N418 |

| | | |
|---|---|---|
| MHC-II-APC | eBioscience | M5/114.15 |
| Cd62L-BV605 | Biolegend | MEL-14 |
| Cd44-FITC | Biolegend | IM7 |
| Cd44-BUV395 | BD | IM7 |
| | | |
| **Virus Strains** | | |
| oHSV | Oncorus | ONCR2 |
| $oHSV^{ULBP3}$ | Oncorus | ONCR7 |
| nrHSV | Oncorus | FDN17 |
| | | |
| **Chemicals and Recombinant Proteins** | | |
| Rat $IgG_2a\kappa$ (isotype control for anti-PD-1) endotoxin low | BioXcell | BE0089 |
| Rat $IgG_2b\kappa$ (isotype control for anti-PD-L1) endotoxin low | BioXcell | BE0090 |
| Mouse $IgG_2b\kappa$ (isotype control for anti-CTLA4) endotoxin low | BioXcell | BE0086 |
| Rat anti-mouse-Pd-L1 mAb endotoxin low | BioXcell | BE0101 |
| Rat anti-mouse-Pd-1 mAb endotoxin low | BioXcell | BE0146 |
| Mouse anti-mouse-Ctla4 mAb endotoxin low | BioXcell | BE0164 |
| D-luciferin | Caliper Life Sciences | #119222 |
| Live/Dead Yellow Amine | Life Technologies | L34968 |
| | | |
| | | |
| **Commercial Assays** | | |
| Fugene 6 transfection kit | Roche | E2691 |
| QIAGEN RNeasy FFPE kit | Qiagen | 73504 |
| nCounter Mouse immunology panel | Nanostring | XT-CSO-MIM1-12 |
| nCounter Mouse myeloid innate immunity panel | Nanostring | XT-CSO-MMII2-12 |
| LDH release assay kit | Roche | 11 644 793 001 |
| AllPrep RNA/Protein kit | Qiagen | 80404 |
| | | |
| **Experimental Models: Cell Lines** | | |
| DF-1 Chicken fibroblast cell line | ATCC | CRL-12203 |
| Primary mouse derived glioblastoma cells | This paper (*N/tva;Cdkn2a*$^{-/-}$*;Pten*$^{fl/fl}$*:PDGFB,Cre*) | N/A |
| | | |
| **Experimental Models: Organisms/Strains** | | |
| *Tg(NES-TVA);Cdkn2a (Ink4a-Arf)*$^{-/-}$*;Pten*$^{fl/fl}$*; LSL Luciferase* | This paper | N/A |
| | | |

| Recombinant DNA | | |
|---|---|---|
| RCAS-HA-PDGFB | Ozawa et. al 2015, Eric Holland | N/A |
| RCAS-Cre | Ozawa et. al 2015, Eric Holland | N/A |
| RCAS-shPten_2 | Ozawa et. al 2015, Eric Holland | N/A |
| | | |
| **Software** | | |
| Prism 7 | GraphPad | N/A |
| FlowJo | Tree star | N/A |
| nSolver | Nanostring | N/A |
| R | R-project | N/A |
| Image J | NIH | N/A |

**Note S1 – Optimizing oHSV attenuation for the treatment of brain tumors**

oHSV strains are among the most thoroughly studied oncolytic viruses, because their DNA-genome renders them genetically stable, their large size enables integration of several transgenes, and the vector immunogenicity limits systemic infection and provides a margin of safety (1). However, neurotropism of wildtype HSV requires attenuation in order to prevent destruction of healthy brain tissue. The most commonly utilized strategy for HSV-attenuation is deletion of the gene encoding the neurovirulence factor ICP34.5 (1). A caveat of this approach is that loss of *ICP34.5* sensitizes oHSV-infected cells to interferon-mediated repression of viral replication and spreading (2). In patients, this limitation can be compensated by repeat intratumoral oHSV injections. For brain tumors, this approach is challenging and the use of a potently replicating oHSV is desirable. As an alternative to *ICP34.5* deletion, we included multiple response elements for the brain abundant tumor suppressor miR-124 into the 3' untranslated region of the gene encoding infected cell protein (ICP)4, a transcription factor essential for HSV replication (3)(Figure S2A).

Mouse glioblastoma cell lines derived from XFM-Luc:PDGF,Cre glioblastomas were lysed when exposed to increasing oHSV doses for 72 hours ($p<0.001$, Figure S2B). To determine the specificity of miR-124 attenuation, we first performed co-immunofluorescence staining upon intratumoral injection in XFM-Luc:PDGF,Cre mouse glioblastomas. The enhanced green fluorescent protein (eGFP), which is expressed with the *UL44* gene to mark viral replication, was not detected in neurofilament stained neurons (Figure S2C). Instead, eGFP was predominantly detected in the Olig2+ population, which comprises mostly glioblastoma cells, and in a subset of Iba1+ TAMs

(Figure S2D). eGFP labeling of TAMs could either be due to infection or to phagocytosis of Olig2-expressing tumor cells by the TAMs. To further explore this issue and determine if oHSV-infected tumor cells showed enhanced phagocytosis by TAMs, we isolated $Cd45^{high}$;Cd11b+;$Ly6c^{low}$ TAMs from untreated XFM-Luc:PDGF,Cre glioblastomas for co-incubation with dye-labeled tumor cell lines derived from the same model (1:1 ratio, 3 hours). Subsequent flow cytometry determined that overnight oHSV infection enhanced phagocytosis of dye-labeled tumor cells by approximately 3-fold (Figure S2E).

In XFM-Luc:PDGF,Cre mice not infected with RCAS vectors, intracranial injection of miR-124-attenuated oHSV at doses of $3x10^6$ plaque forming units (PFU, N=23 mice), but not of $1x10^6$ PFU (N=14) induced transient shivering and lethargy for up to three days. These symptoms resolved in all cases and never resulted in death, persistent neurologic symptoms or histologic signs of encephalitis. In all subsequent experiments, oHSV treatment was performed with $1x10^6$ PFU injected directly into tumors utilizing the identical coordinates as for RCAS injection to initiate tumor formation. We conclude that intracranial injection of miR-124-attenuated, $ICP34.5^{+/-}$ oHSV was a safe and tumor cell specific approach to enhance phagocytosis by TAM.

**Supplemental References**

1. Lawler SE, Speranza MC, Cho CF, and Chiocca EA. Oncolytic Viruses in Cancer Treatment: A Review. JAMA Oncol. 2017;3(6):841-9.

2. Mossman KL, and Smiley JR. Herpes Simplex Virus ICP0 and ICP34.5 Counteract Distinct Interferon-Induced Barriers to Virus Replication. Journal of Virology. 2002;76(4):1995-8.

3. Mazzacurati L, Marzulli M, Reinhart B, Miyagawa Y, Uchida H, Goins WF, Li A, Kaur B, Caligiuri M, Cripe T, et al. Use of miRNA response sequences to block off-target replication and increase the safety of an unattenuated, glioblastoma-targeted oncolytic HSV. Mol Ther. 2015;23(1):99-107.

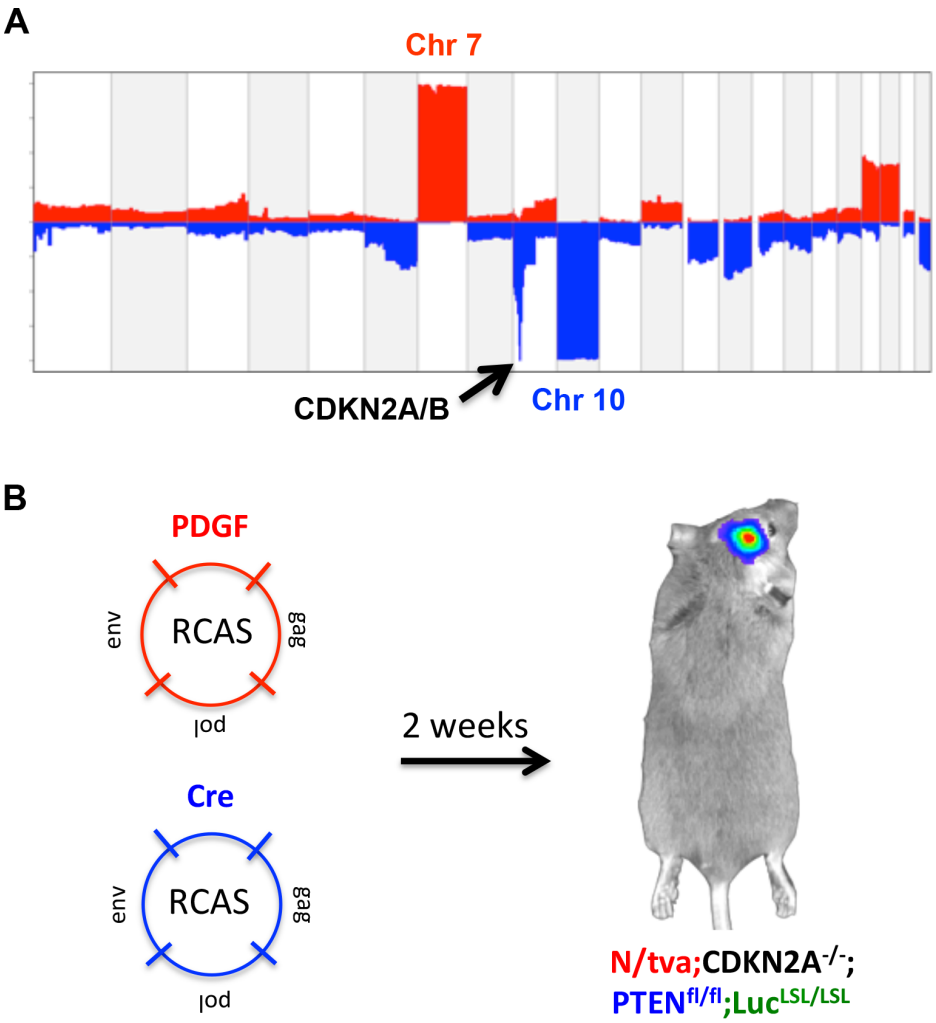


**Figure S1. XFM-Luc:PDGF,Cre mouse glioblastomas recapitulate molecular features of human glioblastoma. A.** Genome plot visualizing frequencies of copy number gains (red) and losses (blue) along the genome in IDH wildtype, *Cdkn2a*$^{-/-}$ human glioblastoma. **B.** RCAS vectors utilized for infection of *NES+* brain cells in indicated transgenic mice.

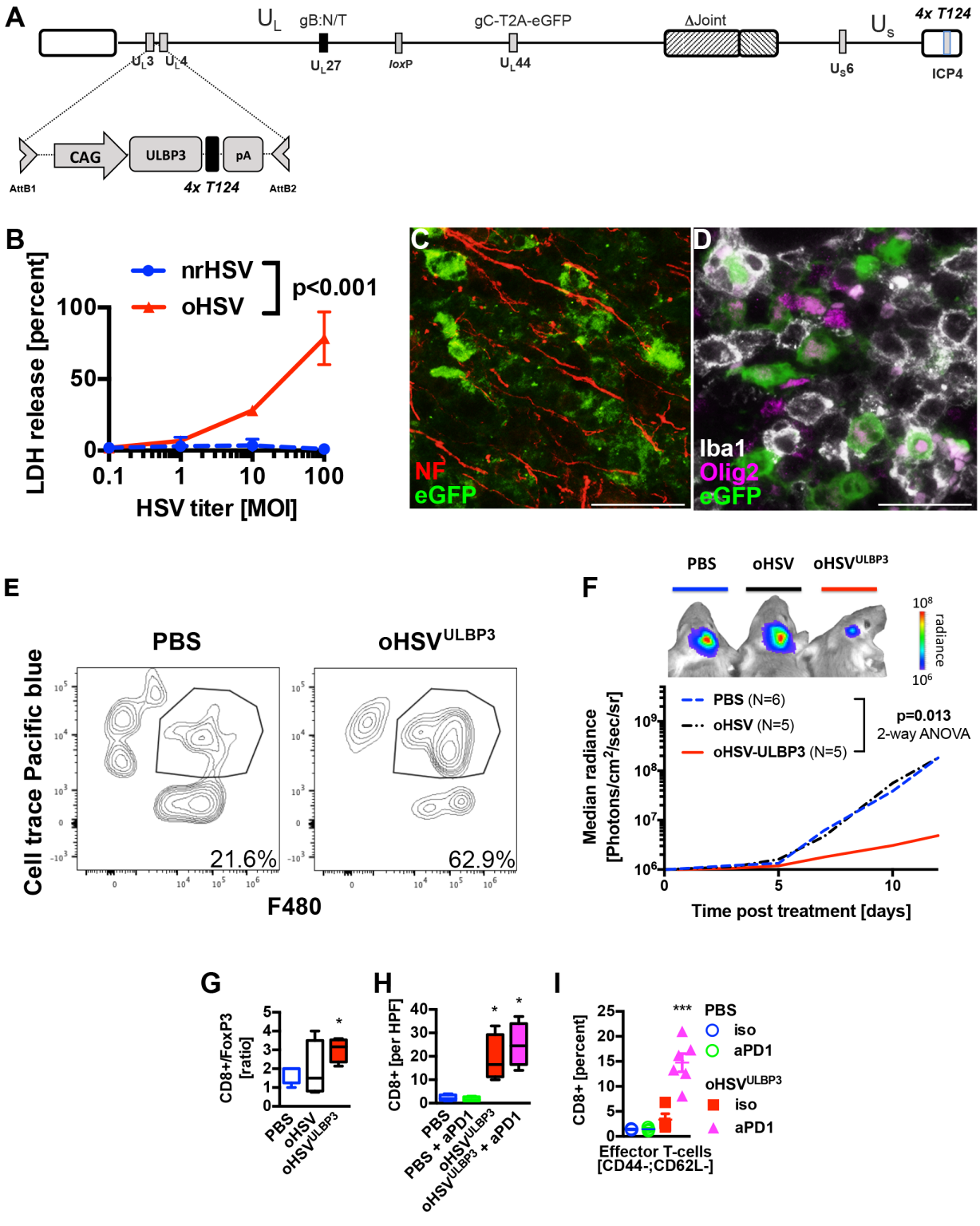


*Figure S2, continued on next page*

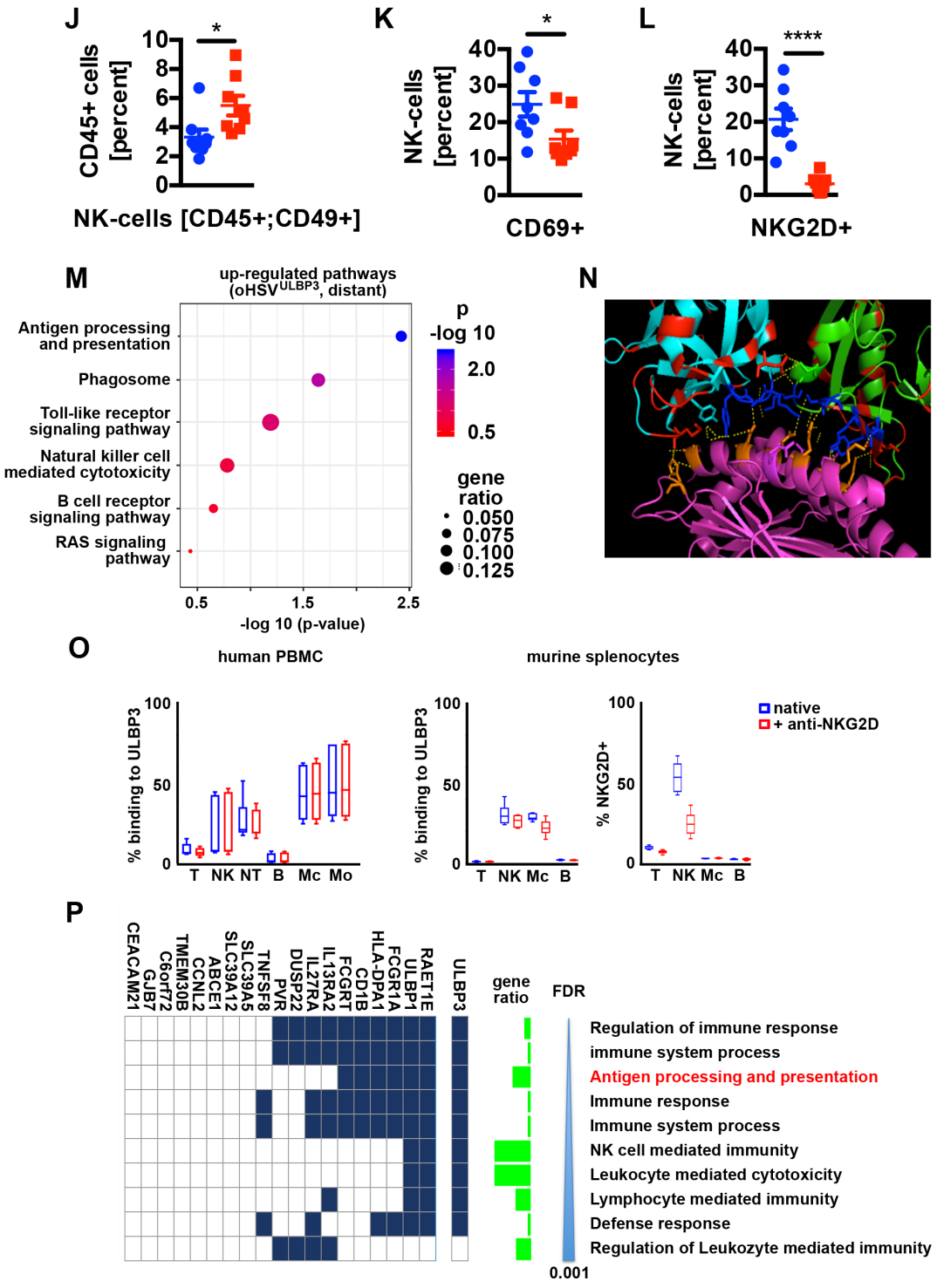


*Figure S2, legend on next page*

**Figure S2. miR-124-attenuated oHSV lyses tumor cells and promotes phagocytosis, and arming oHSV with ULBP3 promotes antigen processing and presentation in an NKG2D and NK-cell independent manner. A.** Vector map of oHSV$^{ULBP3}$. *T124*, miR-124 response elements. **B.** Left panel: dose-response of the lytic potential of the oHSV backbone in primary mouse glioblastoma cells derived from XFM-Luc:PDGF,Cre tumors. LDH release is expressed as percentage of triton-lysed cells (N=4 technical replicates). nrHSV, non-replicating HSV-strain (FDN17). Cells were infected 48 h prior to analysis. MOI, moiety of infection. Right panel: representative fluorescence microscopic image of XFM-Luc:PDGF,Cre cells infected with 100 MOI oHSV; eGFP detection marks viral replication. **C, D.** XFM-Luc:PDGF,Cre glioblastomas were injected with miR-124-attenuated oHSV ($1x10^6$ PFU) on day 14 after tumor initiation and were sacrificed on day 21. eGFP marks viral replication. Olig2 marks predominantly tumor cells. Co-immunofluorescence stainings were done for **(C)** eGFP and neurofilament (NF), and **(D)** eGFP, Iba1 and Olig2. Scale bar, 50 μm. **E.** Flow cytometry of XFM-Luc-derived TAM co-incubated for 4 h with dye-labelled XFM-Luc glioblastoma cells (1:1 ratio, 3 hours). Cancer cells were infected with 10 MOI oHSV or treated with PBS overnight. Percentages indicate the fraction of macrophages that were double-positive for the TAM marker F480, and for the cell tracer pacific blue, indicating phagocytosis of cancer cells. **F.** Bioluminescence imaging of tumor growth. XFM-Luc:PDGF,Cre mouse glioblastomas were treated as indicated on day 14 after tumor initiation. Luciferin emission was measured every 2-3 days. Upper panel: representative measurement; lower panel: median tumor growth. **G.** Ratios of the maximal number of Cd8+ over FoxP3+ cells per high power field (HPF, 40x) in tissue slides of mice sacrified on day 7 after indicated treatment determined by immunohistochemistry (N=4 mice/group). **H.** Counts of Cd8+ cells (N=4 mice/group) of mice sacrified on day 7 after initiation of indicated treatments and stained by immunohistochemistry. aPD1, anti-PD-1 10 mg/kg i.v. every other day; iso, IgG isotype control. **I.** Flow cytometry of the Cd8+ effector T-cell fractions on day 7 (N=6-8 mice/group). **J-L.** Flow cytometry of whole tumors treated with PBS or oHSV$^{ULBP3}$ (N=8 mice/group) of mice sacrified on day 7 after initiation of indicated treatments. * $p<0.05$, **** $p<0.001$. **M.** nCounter myeloid gene expression analysis of tumor-bearing mouse brain hemispheres treated with oHSV$^{ULBP3}$ or PBS followed by geneset enrichment analysis of gene ontology (GO) terms annotated to biological processes. **N.** Three-dimensional structure of ULBP3 and NKG2D. The protein modeling portal was accessed to explore interactions of ULBP3 with mouse and human NKG2D. Human NKG2D forms a homodimer (cyan, green) with ULBP3 (magenta). Amino acids that differ with mouse NKG2D are shown in red, amino acids involved in the interaction surface are shown in blue/orange and polar contacts between chains are depicted with yellow dashes. **O.** Flow cytometry to determine interactions of Fc-tagged ULBP3 with immune cells in the presence or absence of anti-NKG2D blocking antibodies in human peripheral blood mononuclear cells (PBMC) from N=3 healty donors (left panel) and splenocytes from N=3 wildtype C57/bl6 mice (middle panel). The presence of NKG2D was determined on mouse splenocytes (right panel). T, T-cells; NK, NK-cells; NT, NKT-cells; B, B-cells; Mc, macrophages; Mo, monocytes. **P.** Gene/geneset overlap matrix of ULBP3 interaction partners (Huttlin et al. 2017) with GO biological process genesets was generated utilizing the open access gene set enrichment software deposited with the MSigDB database v6.2 from Broad Institute. FDR, false-discovery rate.

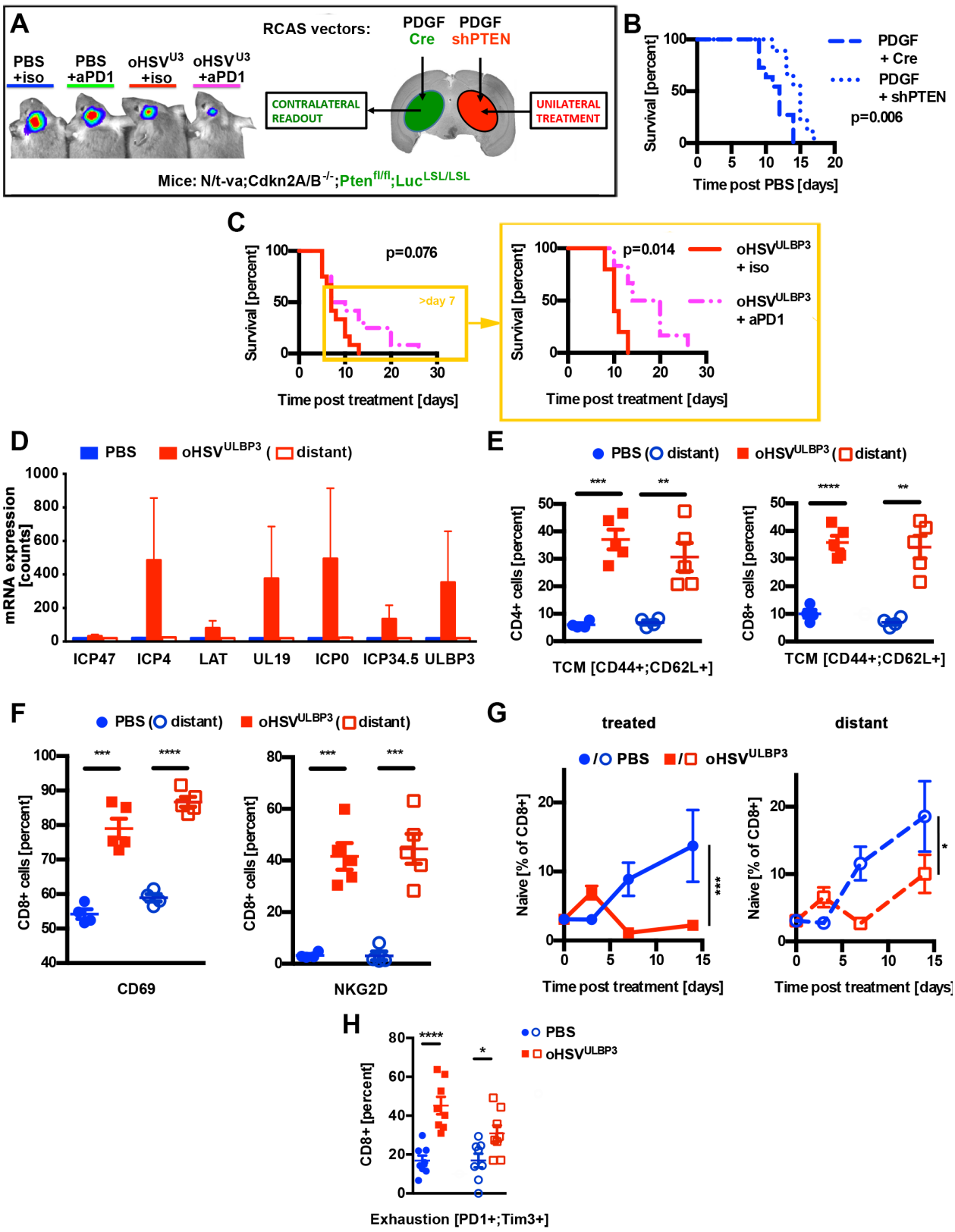


*Figure S3, legend on next page*

**Figure S3. Localized oHSV$^{ULBP3}$ infection elicits a distant immune response and sensitizes distant tumor lesions to anti-PD-1. A.** Schematic of the bilateral XFM-Luc:PDGF,Cre/shPten tumor model utilized for bioluminescence imaging of distant (abscopal) tumor growth (right panel) and representative images from day 10 after initiation of indicated treatments. aPD1, anti-PD-1; iso, IgG isotype control. Treatment schedule as in Figure 4A. **B.** Survival of XFM-Luc mice bearing unilateral PDGF-driven tumors co-transduced with RCAS-Cre (N=11) or RCAS-shPten (N=9). **C.** Survival of XFM-Luc mice bearing bilateral tumors driven by PDGF and Cre/shPten after unilateral treatment with oHSV$^{ULBP3}$ (Figure S4A). Left panel: Indicated treatment groups from Figure 4B (isotype, N=19; anti-PD-1, N=12). Right panel: Only mice surviving $\geq$ 7 days are depicted (isotype, N=5; anti-PD-1, N=6). Kaplan-Meier curves were compared utilizing the log rank test. **D.** Normalized gene expression levels of viral antigens in PBS-treated tumors (negative control), oHSV-infected tumors and in contralateral untreated tumors. A customized nCounter panel was utilized on day 7 after oHSV infection. Unpaired, two-tailed t-test.
E. Flow cytometry to determine the fractions of T central memory (TCM) cells in the tumor infiltrating Cd4+ (left panel) and Cd8+ (right panel) lymphocyte populations in bilateral XFM-Luc:PDGF,Cre tumors. Treated and distant (contralateral untreated) tumor-bearing hemispheres were analyzed separately. N=5 mice per group were analyzed three days after unilateral intratumoral injection of PBS or oHSV$^{ULBP3}$. Unpaired, two-tailed t-test. **F.** Flow cytometry to determine the fractions of activated Cd69+ (left panel) and Nkg2D+ (right panel) tumor-infiltrating Cd8+ lymphocytes in bilateral XFM-Luc:PDGF,Cre tumors. N=5 mice per group were analyzed three days after unilateral intratumoral injection of PBS or oHSV$^{ULBP3}$. Unpaired, two-tailed t-test. **G.** Flow cytometry time-course analysis of the Cd44-;Cd62L+ fraction of naïve tumor-infiltrating Cd45+;Cd3+;Cd8+ lymphocytes in bilateral oHSV-Luc:PDGF,Cre tumors treated unilaterally with PBS (N=6) or oHSV$^{ULBP3}$ (N=8). Left panel: treated hemispheres; right panel: distant hemispheres (contralateral, untreated). Curves were compared by linear regression. **H.** Flow cytometry of mouse glioblastoma-bearing hemispheres 7 days after injection with PBS or oHSV$^{ULBP3}$ (closed symbols, treated), or corresponding contralateral hemispheres (open symbols, distant). Fractions in Cd45+;Cd3+;Cd8+ T-cells positive for both surface exhaustion markers PD-1 and Tim3 are depicted. Unpaired 2-tailed t-test, * $p<0.05$, **** $p<0.0001$.

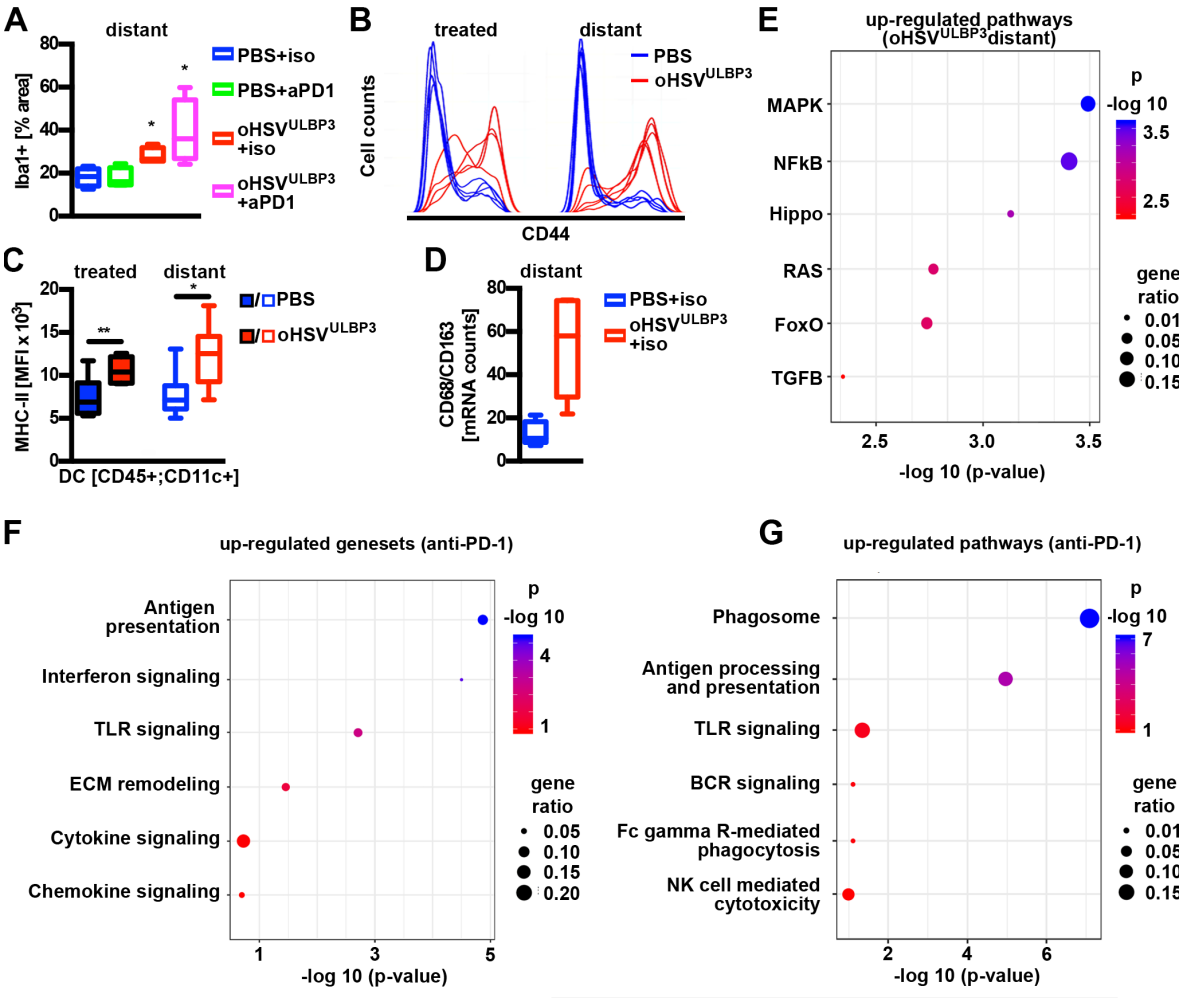


**Figure S4. Anti-PD-1 augments oHSV$^{ULBP3}$ driven abscopal TAM activation. A.** Immunohistochemistry for Iba1 in the contralateral hemispheres upon unilateral treatment with PBS or oHSV$^{ULBP3}$ in combination with anti-PD-1 or isotype 10 mg/kg i.v. every other day. The overall surface covered with Iba1+ cells was determined at low magnification (4x) utilizing Image J. N=4 mice per group. Unpaired, two-tailed t-test. **B.** Flow cytometry normalized histograms depicting the Cd44+ cell population in mouse glioblastoma-bearing hemispheres 14 days after injection with PBS or oHSV$^{ULBP3}$ (left panel), and abscopally in distant untreated tumor-bearing hemispheres from the same mice (right panel). **C.** Flow cytometry to determine the median fluorescence intensity (MFI) of MHC-II on the cell surface of Cd11c+ dendritic cells (DC) in bilateral XFM-Luc:PDGF,Cre tumors. N=6 mice per group were analyzed 7 days after unilateral intratumoral injection of PBS or oHSV$^{ULBP3}$. Unpaired, two-tailed t-test. **D.** Ratio of normalized Cd68/Cd163 mRNA counts determined by nCounter myeloid gene expression panel analysis in contralateral, untreated tumors of the bilateral XFM-Luc:PDGF,Cre model. N=5 mice per group. Unpaired, two-tailed t-test. **E.** Geneset enrichment analysis of up-regulated KEGG pathways abscopally in untreated, distant tumors of unilaterally oHSV$^{ULBP3}$ treated, bilateral XFM-Luc:PDGF,Cre glioblastoma-bearing mice. PBS-treated tumors were utilized as the reference. N=5 mice per group. **F, G.** nCounter myeloid gene expression analysis of tumor-bearing mouse brain hemispheres treated with anti-PD-1 or isotype 10 mg/kg i.v. every other day, followed by geneset enrichment analysis of gene ontology (GO) terms annotated to biological processes (F) or KEGG pathways (G).
* p<0.05, ** p<0.01